Chitosan-Ion Imprinted Polymer Based Modal Interferometer for Ultra-trace Cd^{2+} Detection

Xujie Wang, Abdullah Al Noman, Maoqi Liu and Changyuan Yu, *Fellow*, *Optica*

***Abstract*—A low-cost, easily fabricated, and compact modal interferometric sensor coated with chitosan-cadmium ion imprinted polymer (CS-Cd^{2+}IP) is proposed and experimentally demonstrated for ultra-trace cadmium detection. The interferometer is constructed by sequentially splicing fixed lengths of multimode fiber (MMF) and no-core fiber (NCF) between single-mode fibers (SMFs). The formation of the CS-Cd^{2+}IP layer for specific cadmium binding is achieved by modifying the interferometer surface with a CS-Cd^{2+} compound and 0.2% epichlorohydrin (ECH) solution. The sensor exhibits a linear cadmium sensitivity of 1.1528 nm/parts per trillion (ppt) and a limit of detection (LoD) of 0.0695 ppt within a rapid and stable response range of 0 to 1 ppt. The sensor demonstrates significantly enhanced selectivity towards Cd^{2+} while minimizing responses to other heavy metal ions (HMIs). The effects of environmental factors such as pH and temperature are investigated to minimize measurement errors and improve accuracy. Two additional sensors are fabricated using the same process to demonstrate the reproducibility of the proposed cadmium sensing scheme.**

***Index Terms*—Fiber optic sensor, heavy metal ions, interferometer, chitosan, imprinted polymer, cadmium ions.**

I. Introduction

MOLECULARLY Imprinted Technology (MIT) is a well-established approach for creating polymeric materials with selective recognition sites for specific target molecules. Owing to their custom-designed binding sites, molecularly imprinted polymers (MIPs) enable highly specific molecular recognition based on a 'lock-and-key' mechanism [1], [2]. To date, MIPs have been employed for the selective detection of various analytes, such as pesticides, proteins, and viruses [3], due to their advantages of low cost, simple fabrication process, broad applicability, robust stability, and reusability [4], [5]. Furthermore, researchers have developed ions imprinted polymers (IIPs) for inorganic ions applications derived from principles of MIPs. These polymers function by forming stable complexes between target ions and coordinating ligands [6], [7]. Specifically, the imprinting process involves cross-linking polymerization reaction between the functional monomers and the cross-linking agent in the presence of template ions [8]. IIPs retain the strong specificity and anti-interference capabilities of MIPs, while the presence of coordination bonds promotes the enrichment of trace heavy metal ions (HMIs), making them an ideal choice for HMIs absorption in aqueous systems [9], [10].

Presently, HMIs such as cadmium (Cd^{2+}), lead (Pb^{2+}), copper (Cu^{2+}), zinc (Zn^{2+}), nickel (Ni^{2+}) and chromium (Cr^{3+}) are increasingly discharged into aquatic environments through human activities [11]. Recent estimates indicate that approximately 40% of global lakes and rivers are affected by heavy metal contamination [12]. Among these pollutants, cadmium ions pose particularly severe threats to public health because of their extreme toxicity and potential for bioaccumulation even at trace levels [13]. Human exposure to Cd^{2+} primarily occurs through contaminated domestic water and beverages. These ions preferentially accumulate in renal and hepatic tissues, where they exhibit an exceptionally long biological half-life of 10-30 years [14]. The pathological mechanisms involve reactive oxide species (ROS) once Cd^{2+} accumulated, which induces oxidative stress, cellular damage, and apoptosis, ultimately contributing to various disorders [15]. Several analytical techniques have been developed to address this critical environmental health challenge, for instance, atomic absorption spectroscopy, chemiluminescence assays, and electrochemical methods [16]. Nevertheless, each approach faces significant limitations, including costly instrumentation, prolonged analysis times, poor selectivity and sensitivity, and the risk of contamination during sample preparation [17], [18].

In contrast, optical fiber sensors (OFSs) have attracted significant research attention owing to their particular merits of low cost, high electromagnetic immunity, rapid response, and simple integration features [13], [19], [20]. Over the years, the incorporation of specific coating materials has enhanced the capabilities of OFSs for trace Cd^{2+} detection. In 2022, Li et al. achieved Cd^{2+} detection at concentrations as low as 10^{-12} mol/L by functionalizing a twisted helical fiber (THF) with propylene thiourea, though the resulting probe exhibited limited selectivity [21]. Zhang et al. developed a sensor using air-hole-assisted multicore microstructured optical fiber (AA-MCF) modified with a hybrid hydrogel. The sensor relied on the formation of S-Cd-S coordination structures, achieving a remarkable sensitivity of 7.443×10^{9} nm/(mol/L) and a limit of detection (LoD) of 6.0×10^{-12} mol/L [22]. Fan et al. recently

Manuscript received; revised; accepted; date of current version. This work was supported by the Government Research Fund 15209321 from Hong Kong Research Council. (*Corresponding author: Changyuan Yu and Abdullah Al Noman.*)

Xujie Wang, Maoqi Liu and Changyuan Yu are with the Photonics Research Institute, Department of Electrical and Electronic Engineering, The Hong Kong Polytechnic University, Hong Kong SAR, China (e-mail: changyuan.yu@polyu.edu.hk).

Abdullah Al Noman is with the Optical Fibre Sensors Research Centre, Department of Electronic and Computer Engineering, University of Limerick, Ireland (e-mail: abdullah.noman@ul.ie).

Color versions of one or more figures in this article are available at.

Digital Object Identifier

reported a UiO-66@Allylthiourea-coated spiral fiber grating (SFG) sensor that leveraged the strong chelating ability of allylthiourea groups and attained an impressive cadmium detection limit of 0.57 nM [23]. Although these approaches have enabled high-precision Cd^{2+} detection, they require complex membrane materials and sophisticated fabrication processes since the demand for high selectivity further increases these challenges. However, these problems can be easily addressed through the introduction of chitosan-ion imprinted polymers (CS-IIPs).

Chitosan (CS) is a low-cost, non-toxic and renewable biopolymer derived from deacetylated chitin, which is massively present in crustacean shells and fungal cell walls. The abundant hydroxyl (-OH) and amino ($-NH_2$) groups in CS facilitate efficient adsorption of heavy metal ions via electrostatic attraction and coordination bonds [13]. However, inherent CS suffers from poor stability, limited selectivity and weak mechanical strength, which significantly restricts its practical applications [24]. The combination of CS with MIT offers a unique approach to overcome the limitations mentioned above efficiently and provides excellent selective adsorption capabilities of CS-IIPs toward numerous HMIs [25], [26]. Moreover, the consumption of hydroxyl and amino groups during the cross-linking polymerization reactions in the imprinting process results in limited detection accuracy [27], [28]. Thus, current strategies for detecting trace amounts of cadmium ions typically combine additional functional layers to enhance sensitivity with CS-IIPs employed for their selective recognition. Such as Shen et al. demonstrated an optical microfiber coupler coated with Fe_3O_4@SiO_2@CS-IIP for cadmium sensing [29]. The sensor displayed a sensitivity of 5.119 nm/nM and a LoD of 0.051 nM. A dual-layer coating of cysteamine-modified graphene oxide and CS-IIP was applied by Wang et al. to a Mach-Zehnder interferometer (MZI), enabling functionalized detection of similar metal ions [13]. The sensor exhibited a sensitivity of -0.1211 nm/parts per billion (ppb) and a LoD of 0.2824 ppb. However, the coating process remains complex and costly, highlighting the need to optimize CS-IIPs for a low-cost, easily fabricated OFS with accurate cadmium recognition.

In this study, we propose a compact modal interferometer coated with chitosan-cadmium ion imprinted polymer (CS-Cd^{2+}IP) for ultra-trace cadmium ion detection that achieves a well-balanced combination of high sensitivity and selectivity. The interferometric structure consists of a multimode fiber (MMF) and a no-core fiber (NCF) fused between single-mode fibers (SMFs). The CS-Cd^{2+}IP layer is generated on the NCF surface by sequentially crosslinking a pre-coated CS-Cd^{2+} compound with epichlorohydrin (ECH) and removing the template using ethylene diamine tetraacetic acid (EDTA). The performance of the fabricated probe is validated following systematic optimization of key coating parameters, including the number of CS-Cd^{2+} compound layers, ECH concentration, and processing time. Additionally, the sensor's pH response, temperature crosstalk elimination using an inscribed FBG, and reproducibility are thoroughly evaluated to enhance measurement precision.

II. Sensing Principle and Sensor Fabrication

A. Materials

Chitosan (medium molecular weight), acetic acid (99%), epichlorohydrin (99%), ethylene diamine tetraacetic acid (99.99%), cadmium chloride (99.99%), lead chloride (99.999%), zinc chloride (99.995%), copper nitrate trihydrate (99%), and chromium nitrate nonahydrate (99%) were employed for sensor functionalization and experimental validation. All reagents were obtained from Sigma-Aldrich and dissolved in deionized (DI) water without any additional modifications before usage.

B. Principle, Fabrication and Demonstration of Modal Interferometer

The schematic of the proposed modal interferometer is depicted in Fig. 1(a). As light enters from the lead-in SMF to the MMF segment, the abrupt core diameter mismatch causes beam expansion and excites multiple higher-order modes from the core mode. These modes further propagate through the NCF region, where the absence of a conventional waveguide core significantly enhances the evanescent wave penetration beyond the fiber surface. Upon reaching the NCF-SMF output junction, the transmitting modes partially recombine and couple into the lead-out SMF core with inherent filtering effects [16], [13]. The lead-out optical intensity (I) can be defined by Eq. 1, where I_{co} and I_{cl} refer to the intensity of core mode and cladding modes, Δn_{eff} denotes the effective refractive index (RI) difference between these modes, and λ stands for the wavelength of incident light.

$$I = I_{co} + I_{cl} + 2\sqrt{I_{co}I_{cl}}\cos\left(\frac{2\Delta n_{eff}}{\lambda}\right) \quad (1)$$

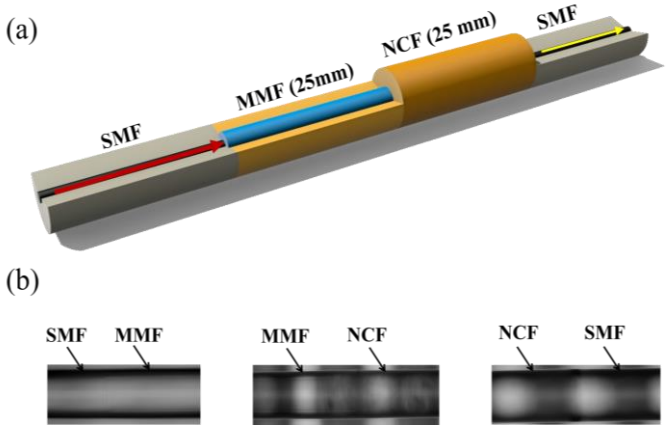

Fig. 1. (a) Schematic diagram of the proposed SMF-MMF-NCF-SMF-based interferometer and (b) microscopic images of fiber splice points.

Changes in the surrounding refractive index directly modulate the effective RI of the cladding modes in the NCF.

Therefore, the phase difference relative to the core-guided modes leads to a shift of the interference fringes in the transmission spectrum. The resulting wavelength shift ($\Delta\lambda_m$) of m^{th}-order interference minima (λ_m) is proportional to Δn_{eff} and the NCF length (L). The relationship can be expressed as [30]:

$$\Delta\lambda_m = \frac{4\Delta n_{eff} L}{(2m+1)^2} \quad m = 1,2,3 \ldots \qquad (2)$$

The interferometer was fabricated using commercial fibers via precise core-to-core fusion splicing process, where 25 mm segments of MMF (60/125 μm) and NCF (125 μm) were spliced in sequence between two SMFs (8.2/125 μm) for input and output connections. The optimized MMF and NCF lengths were adopted from our previous study as the 25 mm configuration demonstrated the highest fringe visibility and strongest main cladding mode distribution in frequency analysis [13]. The splicing procedure was carefully performed using a FITEL S179 fusion splicer in manual mode. Constant arc power was maintained during fusion, while arc durations were varied to achieve high-contrast interferometric minima. Moreover, the microscopic images of each splice region were illustrated in Fig. 1(b). Further, the performance of the proposed structure was evaluated for RI measurement by comparing it with the conventional SMF–NCF–SMF (SNS) structure. The RI values in the range of 1.3320 to 1.4029 were prepared by mixing different concentrations of glycerol solutions with DI water. As shown in Fig. 2, the SMNS achieved a linear sensitivity of 186.57 nm/RIU compared with 150.83 nm/RIU for the SNS, demonstrating an enhancement of over 20% and confirming the superior RI sensing performance of the proposed structure.

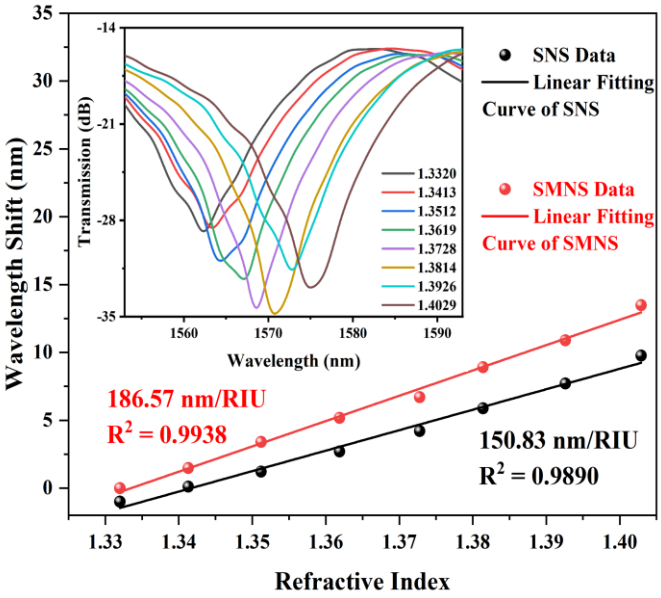

Fig. 2. Linear sensitivity regression of the SNS and SMNS interferometers for RI solutions ranging from 1.3320 to 1.4029. The inset illustrates the interference minima shift of the SMNS interferometer.

C. Coating Process and Ion Exchange Process of CS-Cd^{2+}IP

The Cd^{2+} enrichment was achieved using CS-Cd^{2+}IP as the functional membrane material. The complete attachment process is displayed in Fig. 3(a). The CS-Cd^{2+} compound was prepared by dissolving 2 g of chitosan powder in 100 mL of 4% aqueous acetic acid and stirring continuously for 12 hours at room temperature. 0.1 g of cadmium chloride was subsequently added as the template, and the CS-Cd^{2+} compound was obtained after 4 hours of chelation under the same conditions. Following thorough cleaning of the

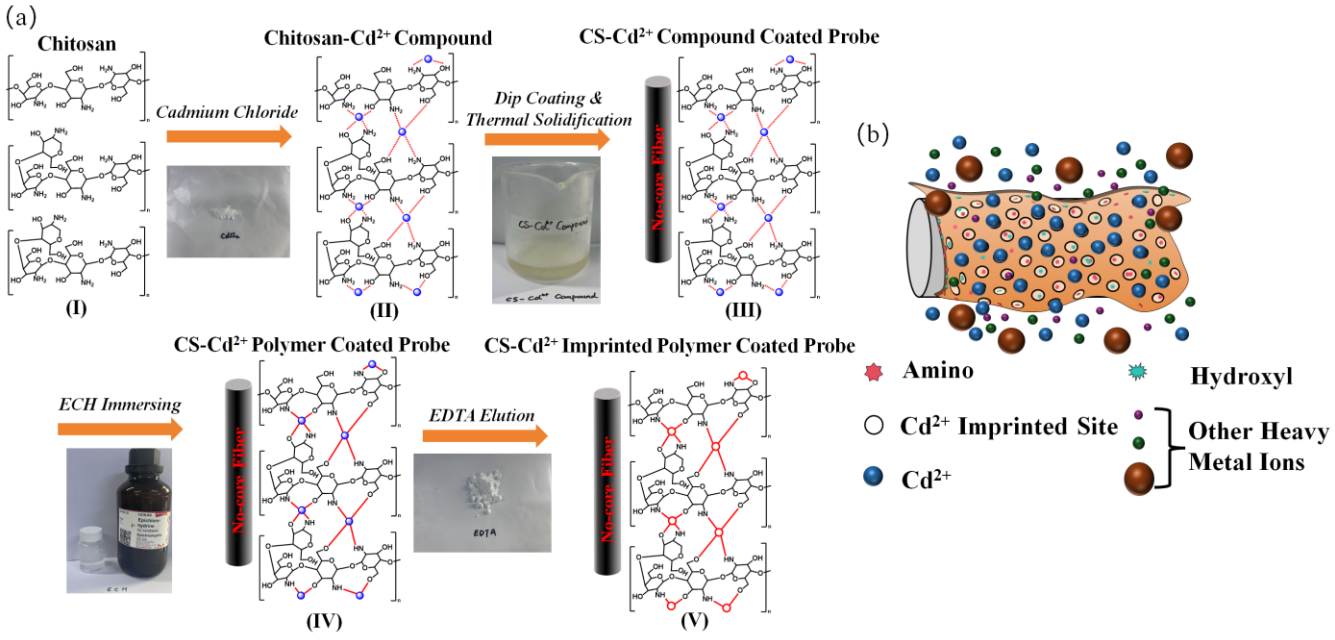

Fig. 3. (a) The complete functional coating process of the CS-Cd^{2+} imprinted polymer, and (b) cadmium recognition process of the CS-Cd^{2+}IP functionalized sensor in external solutions.

interferometer probe with ethanol and DI water, the synthesized material was dip-coated onto the NCF for 5 minutes and thermally cured at 55 °C for 30 minutes. The probe underwent multiple coating cycles to achieve optimal thickness, followed by immersion in ECH to initiate crosslinking polymerization. A dense mesh-like CS-Cd^{2+} polymer structure was formed through chemical bond formation between the -OH and -NH_2 groups of CS [31]. Finally, the template ions were removed by bathing in 0.1 M EDTA because of its high cadmium-chelating ability, thereby creating imprinted sites for sensing [13]. Fig. 3(b) shows the ion-exchange process of the CS-Cd^{2+}IP-coated probe when exposed to solutions containing various HMIs. Although multiple HMIs can bind to amino and hydroxyl groups, the imprinted sites selectively and strongly anchor cadmium ions to the polymer surface. Completion of chelation between active groups and bound Cd^{2+} causes structural compaction of the membrane, leading to measurable changes in external RI that correlate with Cd^{2+} concentration. Ultimately, the interferometer's precise detection of RI changes enables selective cadmium monitoring.

D. Experimental Setup

The experimental setup for real-time monitoring of the interference spectrum during coating optimization and cadmium measurement is depicted in Fig. 4. The CS-Cd^{2+} IP-functionalized interferometer was incorporated into an optical setup featuring a broadband source (BBS, Mingchuang Optoelectronics Co., Ltd.) at the input port and a high-resolution optical spectrum analyzer (OSA, AQ6370D, YOKOGAWA) at the output terminal. Within this setup, light from the BBS expanded in the MMF and coupled into the NCF, where cladding modes interacted with the coated polymer. The lead-out SMF collected the modified phase differences, producing interference patterns on the OSA that reflect membrane properties and cadmium concentrations.

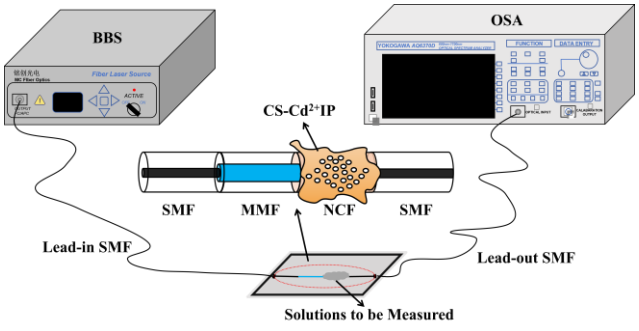

Fig. 4. Experimental setup for sensor optimization and cadmium detection.

III. Experimental Results

A. Optimization of CS-Cd^{2+} Compound Coating Thickness

The coating thickness directly correlates with the number of active sites introduced and significantly affects the chelation capacity for cadmium. Therefore, maximizing the membrane thickness during coating enhances cadmium detection performance. The shape of the interference spectra was monitored after successive cycles of CS-Cd^{2+} compound deposition (see Fig. 5). It can be noted that a significant decrease in interference dip contrast was observed from the fourth cycle onward due to excessive coating layers. Besides, a slight blue shift is observed beyond two layers as the dominant cladding mode enters an anti-resonant regime, reducing the effective index difference with the core and shifting the spectrum to shorter wavelengths. Consequently, three layers of CS-Cd^{2+} compound deposition were selected for further optimization.

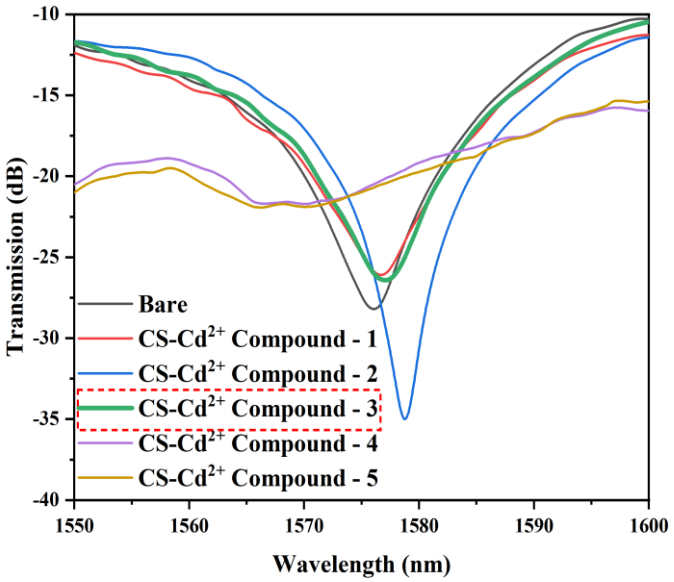

Fig. 5. State of the interference pattern after depositing different CS-Cd^{2+} compound layers.

B. Optimization of ECH Concentration and Immersing Time

Preliminary tests were performed on similarly configured interferometers to optimize ECH concentration. The ECH concentration was chosen between 0.2% (v/v) to 1% (v/v) as higher levels often caused fiber damage and spectral distortion, while lower concentrations failed to form well-defined imprints. To ensure the successful formation of the imprinting polymer for cadmium sensing, the interferometers were immersed in 0.2%, 0.5%, and 1% (v/v) ECH solutions for 6 hours. Following CS-Cd^{2+}IP layer formation on the probe surfaces, three sensors were tested with cadmium solutions ranging from 0 to 10,000 ppb. The spectral shifts of probes prepared with varying ECH concentrations in response to cadmium solutions are shown in Fig. 6. Among the tested probes, the probe with 0.2% ECH demonstrated high sensitivity within the 0 ppb to 10 ppb cadmium concentration range, which can be attributed to its superior preservation of active binding sites. Further, the wavelength exhibits a blueshift due to a nonlinear response arising from saturation of the active binding sites at higher Cd^{2+} concentrations.

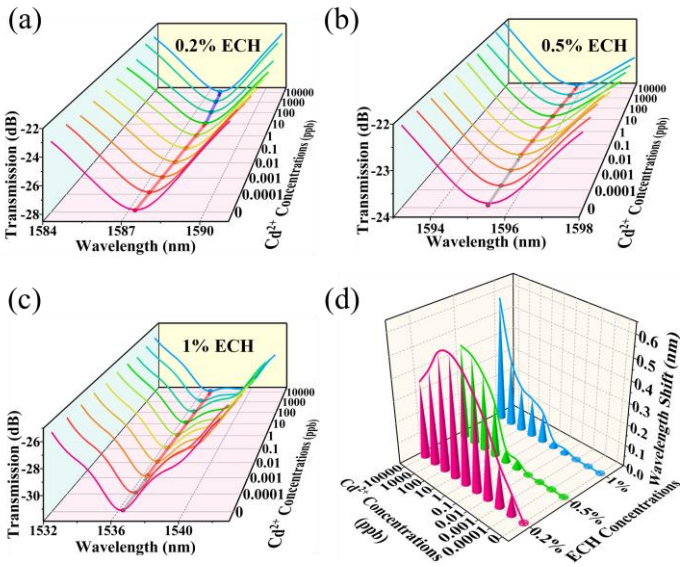

Fig. 6. Spectral response of interferometers to Cd^{2+} concentrations ranging from 0 to 10,000 ppb with ECH treatments at (a) 0.2%, (b) 0.5%, and (c) 1%. (d) Shows the corresponding wavelength shifts for each modified probe.

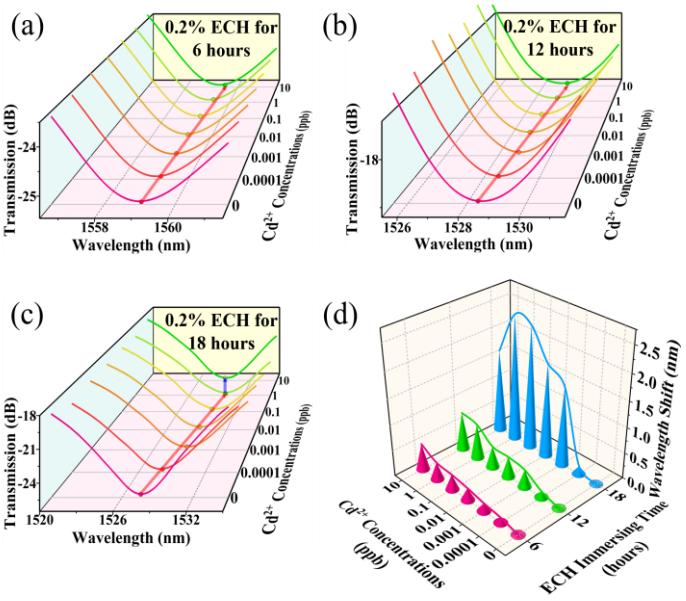

Fig. 7. Interference spectral response of interferometers to Cd^{2+} concentrations from 0 to 10 ppb with 0.2% ECH treatment for different durations: (a) 6 hours, (b) 12 hours, (c) 18 hours, and (d) demonstrates the wavelength shifts of the fabricated sensors treated with 0.2% ECH for different durations.

Afterwards, the ECH immersion time was optimized to enhance both the quantity and quality of cadmium ion imprinted sites. This leads to intensified refractive index changes through denser chelation and enhances sensor sensitivity. Thus, three CS-Cd^{2+} compound-coated probes were immersed in 0.2% ECH for 6, 12, and 18 hours to evaluate their performance in cadmium solutions ranging from 0 to 10 ppb. Fig. 7 shows the spectral responses of the probes coated with ECH at different immersion times. An enhanced sensitivity within the 0-1 ppb cadmium range was observed for the probe with the longest ECH immersion time, thereby designating it as the optimized probe for further analysis. A blue shift appeared beyond 1 ppb as a result of functional group degradation caused by extended ECH treatment. The successful formation of Cd^{2+} imprinted sites on the chitosan surface was confirmed by scanning electron microscopy (SEM). Furthermore, SEM images in Fig. 8 illustrate a smooth and homogeneous coating of Cd^{2}-imprinted CS on the interferometer surface. Therefore, the interferometer pre-coated with three layers of the CS-Cd^{2+} compound and treated with 0.2% ECH for 18 hours was selected as the cadmium sensing probe.

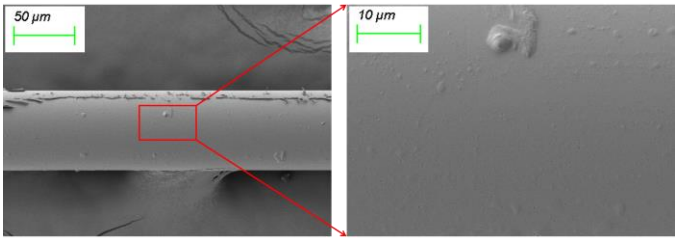

Fig. 8. SEM images of CS-Cd^{2+}IP coated probe.

C. Calibration and Demonstration of Functionalized Sensor

The optimized sensor was further calibrated by sequentially dipping it into cadmium solutions and EDTA to validate the productive chelation capability of the IIP. As shown in Fig. 9(a), each immersion in cadmium caused the interference minima to shift toward longer wavelengths, while subsequent treatment with EDTA followed by DI water restored the minima to its original position. The sensor stabilized within about 10 seconds upon cadmium exposure due to the high density of well-formed imprinted sites and active functional groups. Conversely, the sensor showed a prolonged response time and significant spectral fluctuations at cadmium concentrations above 0.001 ppb. Therefore, the proposed sensor's effective measurement range was defined as 0 to 0.001 ppb (equivalent to 1 part per trillion, ppt) to ensure accuracy and reliability. An average sensitivity of 1.1528 nm/ppt and a LOD of 0.0695 ppt were achieved by the optimized sensor within the specified cadmium concentration range, as depicted in Fig. 9(b). The LOD was determined according to the equation in [20], with σ (σ = 0.0267) denoting the standard deviation and S the average sensor sensitivity. This detection capability is 43165 times more sensitive than the World Health Organization's 3 ppb limit for cadmium in drinking water [13]. A bare SMNS structure was also tested by following the same dipping procedure in cadmium solutions to assess potential crosstalk from ambient RI variations. Fig. 9(a) illustrates that no significant shifts were observed in the interference minima, confirming the response in the functionalized probe is due to the specific binding of Cd^{2+} to the MIP layer.

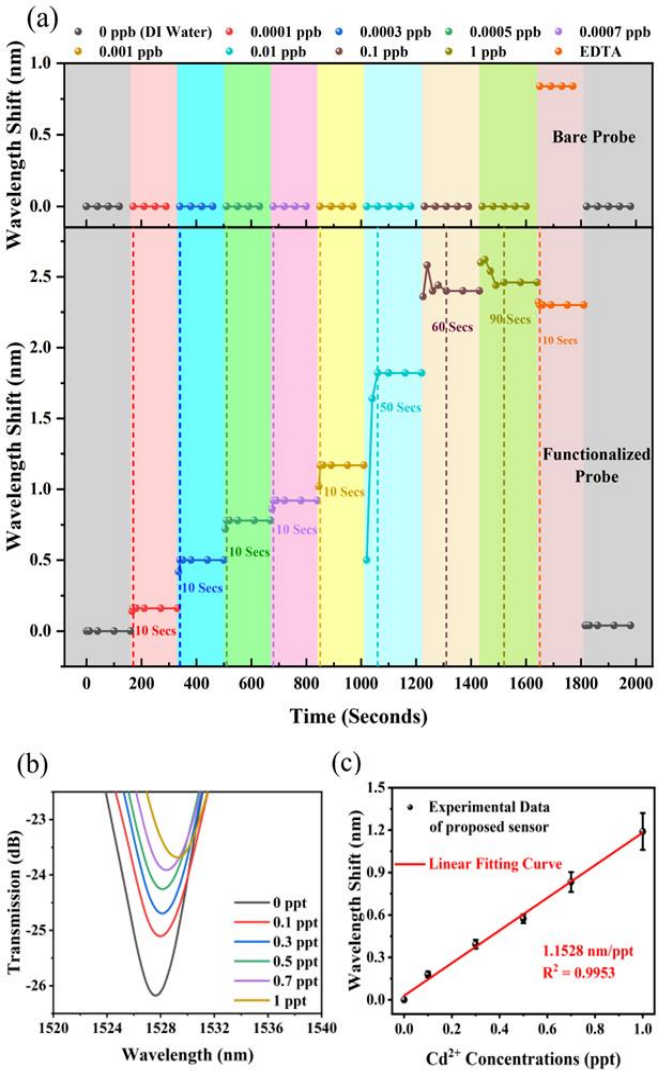

Fig. 9. (a) Response time of a bare probe and the optimized functional probe towards various cadmium concentrations from 0 ppb to 1 ppb and subsequent EDTA regeneration. (b) and (c) Interference minima response and linear sensitivity curve of the optimized probe measured over three repeated cycles in the 0 to 1 ppt cadmium concentration range, respectively.

D. Cadmium selectivity with CS-Cd^{2+} Imprinted Polymer

Moreover, the recognition capability of the CS-Cd^{2+}IP sensor was validated by immersing it in various heavy metal ion solutions, including Pb^{2+}, Zn^{2+}, Cu^{2+}, and Cr^{3+}. The concentration range for all these ions was kept consistent with that of the cadmium detection range to ensure accuracy and comparability. These solutions were prepared by serial dilution from their respective stock solutions. Fig. 10 displays the maximum wavelength shifts of the CS-Cd^{2+}IP modified interferometer compared to the non-imprinted CS-coated sensor in response to various HMIs. It can be seen that the optimized sensor exhibited four times greater sensitivity than the CS-only probe for cadmium detection and achieved an eight-fold enhancement in selectivity over other analytes. These comparative analyses verified the high specificity of the sensor toward cadmium detection.

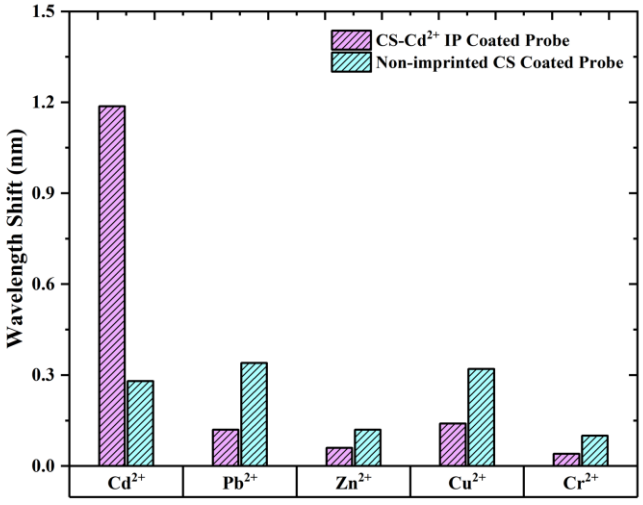

Fig. 10. Selectivity comparison between CS-Cd^{2+}IP-based and non-imprinted CS-based sensors, evaluated by immersing them in various heavy metal ion solutions ranging from 0 to 1 ppt.

E. pH and Temperature Crosstalk Measurement

Mitigating pH and temperature crosstalk is essential to ensure reliable sensor performance in practical applications, since such fluctuations commonly interfere with sensor accuracy. The pH response of the sensor was evaluated over a pH range of 4 to 10, with each measurement performed in triplicate, where the interference dip remains unchanged at pH 7 (see Fig.11). In contrast, deviations in acidity or alkalinity reduced transmission loss and increased crosstalk at the interference minima. This effect is attributed to the protonation or deprotonation of functional groups on the CS-Cd^{2+}IP layer, which alters the refractive index contrast and mode coupling conditions. This compromise in detection accuracy underscores the importance of maintaining near-neutral pH conditions to ensure precise cadmium detection.

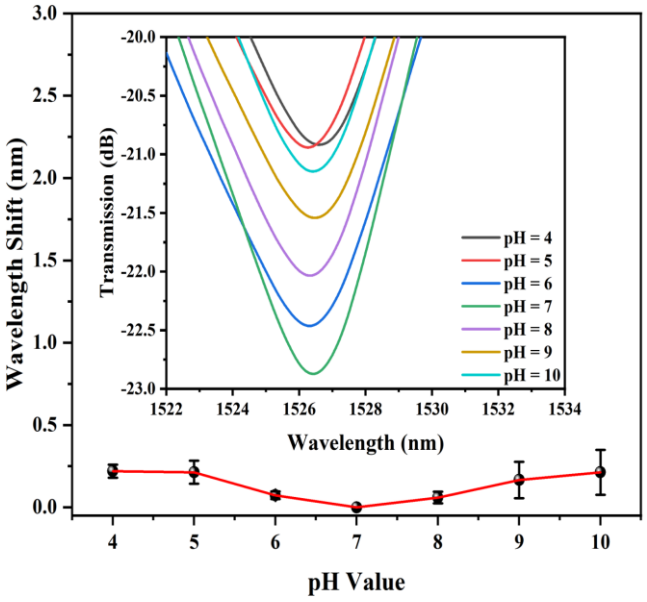

Fig. 11. Spectrum movement evaluated in solutions with pH values from 4 to 10.

TABLE I
COMPARISON WITH DIFFERENT OPTICAL FIBER SENSORS FOR TRACE CADMIUM DETECTION

Structure	Material	Linear Sensitivity (nm/ppt)	Limit of Detection (ppt)	Selectivity	pH Response	Temperature Response (nm/°C)	Ref.
Twisted helical fiber	Propylene thiourea	0.0645	0.1124	No	No	-	[21]
AA-MCF	Hydrogel	0.0662	0.6745	Yes	Yes	0.0183	[22]
SFG	Gold/UiO66@ Allylthiourea	0.0031	64.074	Yes	No	0.3230	[23]
Excessively tilted fiber grating	Hydrogel	0.0943	2.2482	Yes	No	-	[32]
NCF	CS-Cd^{2+}IP	1.1528	0.0695	Yes	Yes	-0.0191	This work

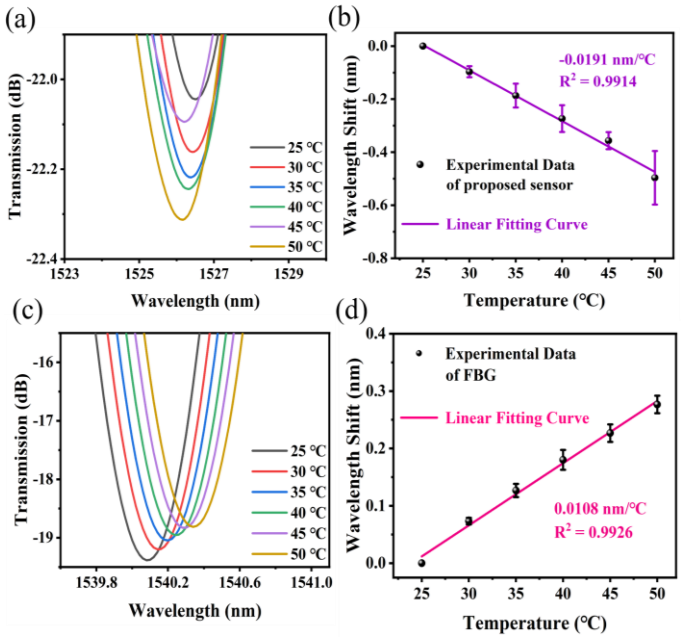

Fig. 12. Spectral shift and linear response to temperature changes from 25 °C to 50 °C, (a, b) for the cadmium sensor, and (c, d) for the embedded FBG.

The effect of environmental temperature variations on the sensor was investigated by observing changes in the interference spectrum, as depicted in Fig. 12. Additionally, a segment of fiber Bragg grating (FBG) was spliced ahead of the coated interferometer to minimize the influence of thermal variations on cadmium sensitivity measurements. Temperature variations from 25 °C to 50 °C were considered in 5 °C increments to measure the sensor's performance. The average temperature sensitivities were measured as -0.0191 nm/°C for the modified interferometer and 0.0108 nm/°C for the FBG peak. Taking cadmium sensitivity into account, the temperature-induced cross-sensitivity was determined to be -0.0166 ppt/°C, which can be effectively compensated using the FBG response. Additionally, Table I provides a comparative summary of recently reported OFSs developed for trace-level cadmium detection.

F. Reusability and Reproducibility

As illustrated in Fig. 13, the reusability of the probe was assessed by alternating cadmium adsorption and EDTA elution within the defined application range.

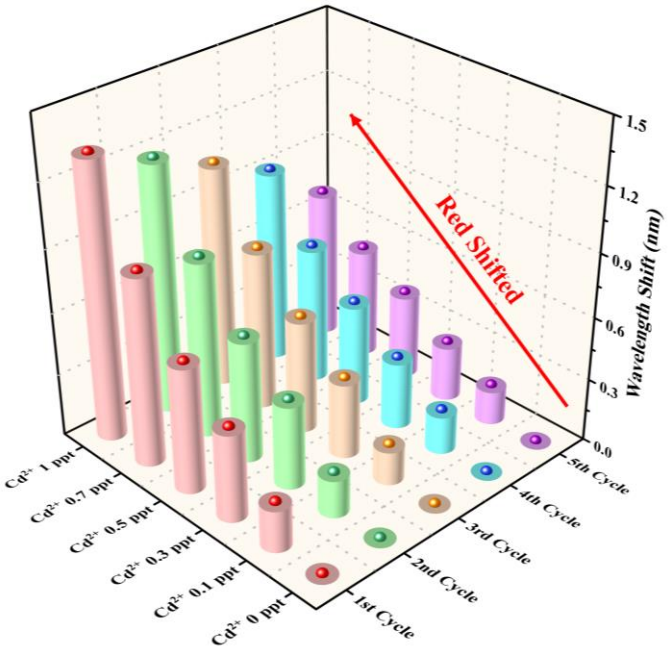

Fig. 13. Reusability of CS-Cd^{2+}IP-coated probe after five maximum cadmium adsorption and EDTA elution cycles.

The findings indicated a gradual decrease in sensitivity over successive testing cycles. The results suggested a gradual decline in sensitivity with successive testing cycles, where the sensitivity decreased to approximately 80% of its original value after three cycles and dropped to around 50% by the fifth cycle. This sensitivity loss can be attributed to the cumulative damage or detachment of imprinted sites induced by repeated cadmium adsorption and elution. The decline is considered an acceptable compromise for achieving low-cost fabrication and high sensitivity. It can be further improved in future studies by introducing stronger crosslinkers (e.g., glutaraldehyde) or optimizing the regeneration protocol.

The reproducibility of the probe was validated by fabricating two identical probes with the same geometry and coating process, as shown in Fig. 14. The sensitivities of these probes to 0-1 ppt Cd^{2+} solutions were 1.1345 nm/ppt (probe 2) and 1.1307 nm/ppt (probe 3), respectively. The detection limits were 0.0238 ppt (σ = 0.0090) for probe 2 and 0.0836 ppt (σ = 0.0315) for probe 3. Despite slight variations arising from differences in membrane uniformity, active site distribution, and imprinted site formation during the functionalization process, the excellent sensitivities and ultra-trace LoDs confirm batch-to-batch reproducibility.

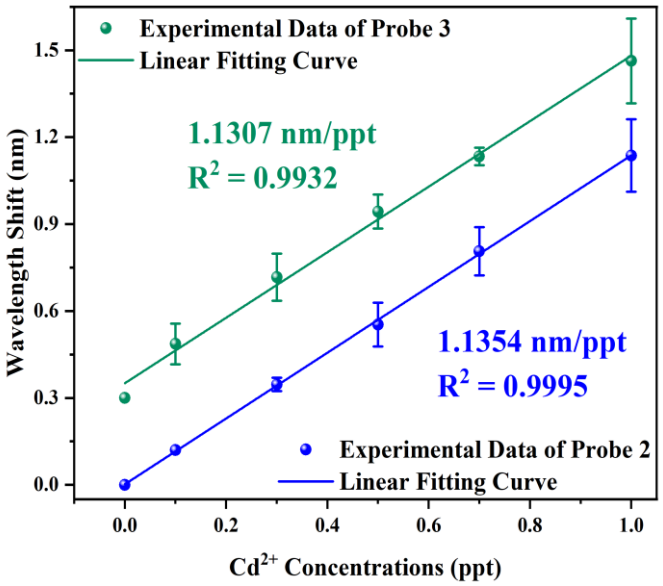

Fig. 14. Linear sensitivities across 0 to 1 ppt cadmium of two identical sensors (probe 2 and probe 3) with the same fabrication scheme, where a 0.3 nm offset was applied on the wavelength shift data of probe 3 to avoid overlap.

IV. Conclusion

This work demonstrates the successful implementation of a CS-Cd^{2+}IP-coated modal interferometer for the highly selective and ultra-trace detection of Cd^{2+} ions. The interferometer is constructed by splicing MMF and NCF segments between two SMFs. The sensor probe is then functionalized through optimized steps, including the deposition of three layers of CS-Cd^{2+} compounds, in situ formation of CS-Cd^{2+}IP using 0.2% ECH for 18 hours, and subsequent EDTA elution. The sensor exhibits an effective cadmium detection range of 0 to 1 ppt with a rapid response time of approximately 10 seconds. An average sensitivity of 1.1528 nm/ppt and a LoD of 0.0695 ppt are achieved by the optimized sensor within the defined range. Compared to the non-imprinted CS-coated probe, it shows a fourfold increase in cadmium sensitivity and significantly reduced responses to other heavy metal ions, confirming its high selectivity. Besides, the optimal pH conditions for minimal crosstalk are found to be near neutral. Additionally, an embedded FBG is integrated to monitor and compensate for thermal effects, resulting in a calculated cross-temperature sensitivity of –0.0166 ppt/°C. Two additional probes were fabricated following the same procedure to validate sensor reproducibility. The cadmium sensitivities and LoDs for the probes are 1.1345 nm/ppt with 0.0238 ppt, and 1.1307 nm/ppt with 0.0836 ppt, respectively. Therefore, the proposed sensor offers a simple yet robust solution for precise cadmium detection in water systems, making it a promising candidate for applications in cadmium stringently controlled scenarios.

References

[1] F. Li, et al., "Application of molecularly imprinted polymers in the water environmental field: A review on the detection and efficient removal of emerging contaminants," *Mater. Today Sustain.*, vol. 27, Sep. 2024, Art. no. 100904.

[2] P. E. Hande, A. B. Samui and P. S. Kulkarni, "Highly selective monitoring of metals by using ion-imprinted polymers," *Environ. Sci. Pollut. Res.*, vol. 22, pp. 7375-7404, Feb. 2015.

[3] M. G. Metwally, A. H. Benhawy, R. M. Khalifa, R. M. El Nashar and M. Trojanowicz, "Application of molecularly imprinted polymers in the analysis of waters and wastewaters," *Molecules*, vol. 26, no. 21, Oct. 2021, Art. no. 6515.

[4] A. Karrat, A. Lamaoui, A. Amine, J. M. Palacios-Santander and L. Cubillana-Aguilera, "Applications of chitosan in molecularly and ion imprinted polymers," *Chem. Afr.*, vol. 3, no. 3, pp. 513-533, Aug. 2020.

[5] J. J. BelBruno, "Molecularly imprinted polymers," *Chem. Rev.*, vol. 119, no. 1, pp. 94-119, Sep. 2018.

[6] L. Rebolledo-Perales, G. Á. Romero, I. Ibarra-Ortega, C. Galán-Vidal and I. Pérez-Silva, "Electrochemical determination of heavy metals in food and drinking water using electrodes modified with ion-imprinted polymers," *J. Electrochem. Soc.*, vol. 168, no. 6, Jun. 2021, Art. no. 067516.

[7] Y. Ma, W. Zheng, Y.-N. Zhang, X. Li and Y. Zhao, "Optical fiber spr sensor with surface ion imprinting for highly sensitive and highly selective ni 2+ detection," *IEEE Trans. Instrum. Meas.*, vol. 70, pp. 1-6, Aug. 2021.

[8] N. F. C. Lah, A. L. Ahmad, S. C. Low and N. F. Shoparwe, "The role of porogen-polymer complexation in atrazine imprinted polymer to work as an electrochemical sensor in water," *J. Environ. Chem. Eng.*, vol. 7, no. 6, Dec. 2019, Art. no. 103500.

[9] X. Zhou, B. Wang and R. Wang, "Insights into ion-imprinted materials for the recovery of metal ions: Preparation, evaluation and application," *Sep. Purif. Technol.*, vol. 298, Oct. 2022, Art. no. 121469.

[10] S. Jakavula, N. R. Biata, K. M. Dimpe, V. E. Pakade and P. N. Nomngongo, "A critical review on the synthesis and application of ion-imprinted polymers for selective preconcentration, speciation, removal and determination of trace and essential metals from different matrices," *Crit. Rev. Anal. Chem.*, vol. 52, no. 2, pp. 314-326, Jul. 2022.

[11] T. K. Sen, "Agricultural solid wastes based adsorbent materials in the remediation of heavy metal ions from water and wastewater by adsorption: A review," *Molecules*, vol. 28, no. 14, Jul. 2023, Art. no. 5575.

[12] V. Singh, et al., "Toxic heavy metal ions contamination in water and their sustainable reduction by eco-friendly methods: Isotherms, thermodynamics and kinetics study," *Sci. Rep.*, vol. 14, no. 1, Mar. 2024, Art. no. 7595.

[13] X. Wang, A. A. Noman, Y. Liu and C. Yu, "Smns structure based fiber optic interferometer for cadmium detection," *Opt. Exp.*, vol. 33, no. 8, pp. 17233-17244, Apr. 2025.
[14] M. A. Arruebarrena, C. T. Hawe, Y. M. Lee and R. C. Branco, "Mechanisms of cadmium neurotoxicity," *Int. J. Mol. Sci.*, vol. 24, no. 23, Nov. 2023, Art. no. 16658.
[15] A. E. Charkiewicz, W. J. Omeljaniuk, K. Nowak, M. Garley and J. Nikliński, "Cadmium toxicity and health effects—a brief summary," *Molecules*, vol. 28, no. 18, Sep. 2023, Art. no. 6620.
[16] X. Wang, A. Al Noman and C. Yu, "Chitosan-ion imprinted polymer-based mach-zehnder interferometer sensors for cd^{2+} detection using cross-linking polymerization," presented at *the 29th Int. Conf. Optical Fiber Sensors*, Porto, Portugal, 2025, pp.257-260.
[17] A. K. Shakya and S. Singh, "State of the art in fiber optics sensors for heavy metals detection," *Opt. Laser Technol.*, vol. 153, Sep. 2022, Art. no. 108246.
[18] Y. Yi, Y. Zhao, Z. Zhang, Y. Wu and G. Zhu, "Recent developments in electrochemical detection of cadmium," *Trends Environ. Anal. Chem.*, vol. 33, Mar. 2022, Art. no. e00152.
[19] A. Al Noman, J. N. Dash, X. Cheng, H.-Y. Tam and C. Yu, "Pcf based modal interferometer for lead ion detection," *Opt. Exp.*, vol. 30, no. 4, pp. 4895-4904, Feb. 2022.
[20] A. A. Noman, et al., "Label-free DNA detection using etched tilted bragg fiber grating-based biosensor," *Sensors*, vol. 23, no. 16, Aug. 2023, Art. no. 7019.
[21] B. Li, et al., "Twist-assisted high sensitivity chiral fiber sensor for cd2+ concentration detection," *Iscience*, vol. 25, no. 10, pp. 105245-105256, Oct. 2022.
[22] A. Zhang, et al., "Trace detection of cadmium (ii) ions based on an air-hole-assisted multicore microstructured optical fiber," *Sens. Actuators B Chem.*, vol. 365, Aug. 2022, Art. no. 131941.
[23] H. Fan, et al., "Uio-66@ allylthiourea film coated optical fiber cadmium ion sensor with spiral grating temperature compensator," *Opt. Fiber Technol.*, vol. 84, May 2024, Art. no. 103731.
[24] S. Ullah, K. Hayat and X. Qiao, "Chitosan-based biostimulation: A novel approach for simultaneous remediation of co-existing cadmium and arsenic contamination in soil," *Air, Soil Water Res.*, vol. 16, Nov. 2023, Art. no. 11786221231216862.
[25] J. Gatabi, Y. Sarrafi, M. M. Lakouraj and M. Taghavi, "Facile and efficient removal of pb (ii) from aqueous solution by chitosan-lead ion imprinted polymer network," *Chemosphere*, vol. 240, Feb. 2020, Art. no. 124772.
[26] A. K. Hajri, B. Jamoussi, A. E. Albalawi, O. H. Alhawiti and A. A. Alsharif, "Designing of modified ion-imprinted chitosan particles for selective removal of mercury (ii) ions," *Carbohydr. Polym.*, vol. 286, Jun. 2022, Art. no. 119207.
[27] N. Li and R. Bai, "A novel amine-shielded surface cross-linking of chitosan hydrogel beads for enhanced metal adsorption performance," *Ind. Eng. Chem. Res.*, vol. 44, no. 17, pp. 6692-6700, Jul. 2005.
[28] M. Vakili, et al., "Regeneration of chitosan-based adsorbents used in heavy metal adsorption: A review," *Sep. Purif. Technol.*, vol. 224, pp. 373-387, Oct. 2019.
[29] T. Shen, et al., "Fiber optic cadmium ion sensors based on functionalization of a magnetic ion-imprinted polymer," *Analyst*, vol. 149, no. 8, pp. 2236-2243, Feb. 2024.
[30] A. Miliou, "In-fiber interferometric-based sensors: Overview and recent advances,"*Photonics*, vol. 8, no. 7, Jul. 2021, Art. no. 265.
[31] L. Xu, Y.-A. Huang, Q.-J. Zhu and C. Ye, "Chitosan in molecularly-imprinted polymers: Current and future prospects," *Int. J. Mol. Sci.*, vol. 16, no. 8, pp. 18328-18347, Aug. 2015.
[32] X. Zhong, W. Zhan, L. Ma and G. Yin, "Trace detection of cadmium (ii) ions based on an excessively tilted fiber grating," *Opt. Exp.*, vol. 32, no. 9, pp. 15851-15861, Apr. 2024.